Active RF Cancellation with Closed-Loop Adaptation for Improved Isolation in Full-Duplex Radios

Active RF Cancellation with Closed-Loop Adaptation for Improved Isolation in Full-Duplex Radios

Adnan Kiayani[†], Mahmoud Abdelaziz[†‡], Dani Korpi[†], Lauri Anttila[†], and Mikko Valkama[†]

[†]*Laboratory of Electronics and Communications Engineering, Tampere University of Technology, FI-33101, Tampere, Finland.*
[‡]*Zewail City of Science and Technology, Giza 12588, Egypt.*
e-mail: adnan.kiayani@tut.fi

***Abstract*—A key challenge in realizing simultaneous radio transmission and reception is suppressing the so-called self-interference (SI) caused by coupling of the own transmitter (TX) signal to the receiver (RX). Moreover, the inherent nonlinearities of the TX and RX front-end components can seriously limit the achievable SI cancellation. In this paper, we present an active radio frequency (RF) cancellation architecture for SI suppression in radio transceivers operating under nonlinear TX power amplifier (PA) and the RX low noise amplifier (LNA). The proposed technique is based on pre-distorting the TX signal to reduce the unwanted PA-induced emissions, and then creating an opposite-phase baseband replica of the linear SI in the transceiver digital front-end through adaptive filtering of the known transmit data. The equivalent RF cancellation signal is finally generated in an auxiliary TX chain and combined with the received signal at the RX LNA input. A closed-loop parameter learning technique, based on the decorrelation principle, is also developed to efficiently estimate both the PA pre-distorter and the digital cancellation filter coefficients in a flexible manner. Experimental results show that the proposed scheme can achieve up to 50 dB SI suppression at the RX LNA input, even at high TX output power and with wide transmission bandwidth, thereby enabling improved TX-RX isolation while reducing the linearity requirements of RF components in in-band full duplex (IBFD) radios.**

***Index Terms*—Adaptive cancellation, digital pre-distortion, flexible duplexing, full-duplex, transmitter leakage signal, self-interference, RF cancellation, nonlinear distortion, 5G.**

I. Introduction

To cater ever growing demands for higher data rates, numerous efforts have recently been made to improve and enhance the radio frequency (RF) spectrum utilization. In-band full duplex (IBFD) communication is considered one of the most promising techniques due to its potential to achieve increased spectral efficiency and reduced communication latency [1], [2]. Compared to the traditional systems that use dedicated resources for transmission and reception either in time or in frequency, IBFD communication enables simultaneous transmission and reception on the same frequency, thus increasing the spectral efficiency by up to two times.

The main challenge when transmitting and receiving simultaneously on the same frequency is the coupling of a strong transmitted signal into the receiver (RX) input. This is referred to as self-interference (SI) which, in addition to IBFD systems, can be a problematic issue also in traditional frequency division duplex (FDD) transceivers operating with a small duplex distance [3], [4], [5], [15]. The presence of such a strong SI can substantially complicate the recovery and detection of the actual received signal-of-interest. Therefore, simultaneous transmission and reception relies on efficient cancellation of the SI to the noise floor level.

In general, it is desirable to suppress the SI before the RX low noise amplifier (LNA), in order to prevent the saturation and generation of nonlinear distortion products in the RX RF front-end components. In this context, two RF cancellation topologies, namely digitally-assisted auxiliary transmitter (TX)-based architecture, and the magnitude and phase adjustment-based pure analog RF cancellation architecture, have been widely discussed in the literature [5] - [15]. These cancellation architectures typically complement the elementary passive RF isolation stage, that is achieved either through a duplexer, circulator, or the like in a shared antenna system, or through proper antenna isolation in a separate antenna system. The digitally-assisted auxiliary TX-based architecture builds on first identifying the *coupling channel* response, referring to the overall response from the TX input to the RX input, and then creating a baseband digital replica of the equivalent RF SI signal through appropriate pre-processing or filtering of the known transmit data. The RF cancellation signal is then generated in the auxiliary TX chain and finally combined with the received signal at the RX LNA input. In contrast, pure analog/RF cancellation approach reproduces the SI signal in the transceiver RF front-end, through proper magnitude and phase adjustment of the PA output signal, and taps it into the RX input.

In this paper, we employ the auxiliary TX-based RF

This work was supported by the Academy of Finland (under the projects #304147 and #301820), the Finnish Funding Agency for Innovation (Tekes, under the project "5G Transceivers for Base Stations and Mobile Devices (5G TRx)"), Nokia Bell Labs, RF360, Pulse, Sasken, and Huawei Technologies, Finland.

cancellation approach, due to its simplicity and improved cancellation gains, to suppress the SI [5]- [11]. However, the hardware imperfections, such as nonlinear distortion and noise generated in the TX chain, also generally contribute to the overall SI appearing at the RX input. These impairments may impose severe limitations on the achievable amount of SI suppression. In particular, the nonlinear distortion products induced by the TX power amplifier (PA) have been shown to be most prominent. In order to maximize the cancellation gain, several recent works have reported nonlinear digital and RF cancellers [5], [9], [10], [11]. While existing nonlinear RF cancellation methods exhibit improved performance for high power and wide bandwidth signals, these techniques typically require a wideband auxiliary TX chain for generating the RF cancellation signal. Moreover, existing techniques rely on complex behavioral modeling of the time-varying SI channel, which leads to a significant increase in the complexity and power consumption of the RF canceller. In contrast, in this paper, we propose to control the PA unwanted emissions through digital pre-distortion (DPD) linearization, by augmenting an observation receiver chain to facilitate DPD parameter learning, while a linear RF canceller suppresses the SI. The closed-loop parameter learning used for both the DPD and the RF cancellation parameter estimation is based on the decorrelation principle, which has been demonstrated, in the authors' earlier works in [5], [16], to be highly efficient and computationally feasible. Moreover, the proposed parameter learning algorithm can also cope with potential nonlinear distortion in the RX LNA during the digital cancellation filter coefficients learning phase, thus offering enhanced RF cancellation. The performance of the proposed technique is evaluated through practical RF measurements, verifying that the proposed technique can provide substantial improvement in the overall TX-RX isolation while also relaxing the RX linearity requirements in IBFD radio systems.

The rest of this paper is organized as follows. In Section II, we present essential signal models for the nonlinear PA-induced distortion and SI, along with the proposed DPD processing and active RF cancellation solution. Then, in Section III, the closed-loop decorrelation-based parameter learning solution is discussed, and the involved computational complexity is analyzed. The RF measurement results are presented and analyzed in Section IV, while concluding remarks are given in Section V.

II. Proposed Transceiver Architecture and SI Cancellation Mechanism

Fig. 1 shows the proposed radio transceiver architecture, with the corresponding processing and active RF cancellation structures. The transceiver is equipped with additional transmitter and receiver chains - an auxiliary transmitter and an observation receiver. The observation receiver provides a baseband replica of the PA output signal, which is used to facilitate the DPD parameter learning. On the other hand, the auxiliary transmitter chain outputs the RF cancellation signal, which is an opposite-phase replica of the SI originally created

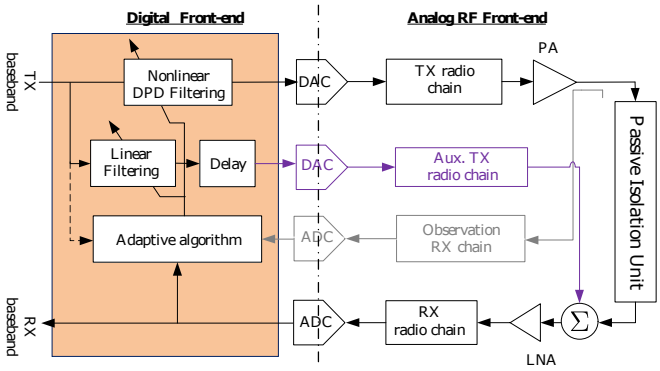

Fig. 1. The proposed architecture of the simultaneous transmit-receive radio transceiver, employing a digital pre-distorter to linearize the TX PA and active RF canceller for suppressing the TX leakage signal.

in the transceiver digital front-end, and combines it with the received signal at the RX LNA input.

In the following subsections, we develop essential signal models for the TX PA DPD and the linear SI canceller, and building on that, the nonlinear and linear digital processing stages are formulated.

A. TX Nonlinear Distortion Modeling and DPD

We denote the baseband transmit signal by $x[n]$. By utilizing the memory polynomial (MP) model, which is widely used for PA modeling and DPD processing, the baseband equivalent PA output signal, yet without DPD, can be written as

$$x_{\text{PA}}[n] = \sum_{\substack{p=1 \\ p\ odd}}^{P} f_{p,n} \star \underbrace{x[n]\,|x[n]|^{p-1}}_{\psi_p[n]} \tag{1}$$

where P is the highest considered nonlinearity order, $f_{p,n}$ denotes the $pth-$order MP branch filter impulse response, $\psi_p[n]$ is the $pth-$order nonlinear basis function, and $\star$ denotes the convolution operator. In general, the PA nonlinearity results in the nonlinear distortion at and around the main transmit carrier, and it is sufficient to consider only odd-order basis functions for modeling the PA-induced nonlinear distortion.

Among different PA linearization techniques, DPD linearization has been recognized as one of the most effective techniques. DPD linearization aims to reduce the PA nonlinear distortion by applying a nonlinear function at the PA input. The response of this nonlinear function is an approximate inverse of the PA nonlinear response, such that the cascaded DPD-PA response is approximately linear. Thus, with an objective to reduce the PA nonlinear distortion at and around the main transmit carrier, the output signal of the DPD reads [16]

$$x_{\text{DPD}}[n] = \sum_{k\in I_k}^{K} h_{k,n} \star \psi_k[n]; \qquad I_k = \{3, 5, \cdots, K\}, \tag{2}$$

where $h_{k,n}$ denotes the $kth-$order DPD filter, with K being the highest DPD nonlinearity order.

B. Linear Digital Processing-Based RF Canceller

The transmit signal, after PA amplification, propagates towards the antenna but, due to limited passive isolation, partially couples into the RX chain and eventually becomes the self-interference. In order to suppress the SI at the LNA input, a baseband replica of the SI can be created in the digital baseband through digital filtering of the known transmit data, to incorporate the effects of passive isolation on the transmit signal. The equivalent RF signal is then created in an auxiliary TX branch, which is finally combined with the received signal at the LNA input. In general, such digitally-assisted RF cancellation techniques can yield better estimates of the coupling channel response over a larger bandwidth, as all the involved processing takes place in the digital baseband.

Hence, the baseband equivalent signal at the combiner output, after RF cancellation, can be written as

$$z[n] = r[n] + \hat{x}_{\mathrm{SI}}[n], \tag{3}$$

where $r[n] = x_D[n] + x_{\mathrm{SI}}[n] + \upsilon[n]$ represents the total received signal that is composed of the desired signal-of-interest $x_D[n]$, the SI $x_{\mathrm{SI}}[n]$, and the thermal noise $\upsilon[n]$. Furthermore, $\hat{x}_{\mathrm{SI}}[n]$ represents the baseband equivalent RF cancellation signal that is combined with the received signal at the LNA input in order to suppress the SI, and can be expressed as

$$\hat{x}_{\mathrm{SI}}[n] = \hat{w}_n \star x[n-\tau]. \tag{4}$$

Here, $\hat{w}_n$ denotes the estimated linear digital cancellation filter impulse response, and τ accounts for the propagation delay introduced by the analog stages to ensure synchronous RF cancellation. The propagation delay is typically fixed and can be estimated offline, prior to performing the RF cancellation. On the other hand, the coefficients of the linear digital cancellation filter, as well as those of the digital pre-distorter, need to be estimated, which is addressed next in the following section. Note that in (3) we have deliberately expressed the cancellation through addition, instead of subtraction, to reflect the operation of an actual RF combiner. The proper 180° phase change for the cancellation signal $\hat{x}_{\mathrm{SI}}[n]$, relative to the actual SI, is realized through the digital filter coefficients $\hat{w}_n$.

III. Closed-Loop Parameter Adaptation

The signal models and processing principles in Section II implicate that the coefficients of the DPD filters $h_{k,n}$, and the digital cancellation filter w_n must be estimated for high accuracy PA linearization and efficient SI suppression. To this end, we propose a two-step estimation processing. In the first step, the DPD coefficients are estimated by utilizing the signal from the observation receiver chain. After obtaining the nonlinear DPD filter parameters and activating the DPD unit, the SI signal is observed through the main receiver and the linear digital cancellation filter impulse response is estimated. These are described in the following subsections, together with a short analysis of the involved computational complexity.

A. Block-Adaptive Parameter Learning

For computing friendly but efficient parameter estimation, we propose a closed-loop block-adaptive learning of both the DPD and digital cancellation filter coefficients. In general, the learning rule, resembling the block-adaptive least-mean squares (LMS) solution, is based on minimizing the correlation between linear and nonlinear basis functions, generated from the known transmit data, and the corresponding error signal observed either through the observation RX or through the main RX. However, the basis functions of different orders are strongly *mutually correlated*, and thus they are first orthogonalized with respect to each other to improve convergence properties. Denoting the transformation matrix by $\mathbf{S}$, the orthogonalized basis functions can be defined as

$$\tilde{\Psi}[n] = \mathbf{S}\Psi[n] \tag{5}$$

where $\Psi[n] = \begin{bmatrix}\psi_1[n] & \psi_3[n] & \cdots & \psi_K[n]\end{bmatrix}^T$ is a vector that contains basis function samples at time index n. The transformation matrix $\mathbf{S}$ can be obtained through, e.g., singular value or QR decomposition [17], or alternatively using the eigendecomposition of the covariance matrix of the nonlinear basis functions [19]. From an implementation perspective, the later approach is in general beneficial as the transformation matrix is recomputed only when statistical properties of the TX signal change and thus does not need to be evaluated for each individual TX data symbol.

After obtaining a new set of orthogonalized basis functions and assembling M samples in an estimation block, we collect all the samples and filter coefficients, within a processing block m, into the following vectors and matrices:

$$\begin{aligned}
&I_k \in \{1, 3, \cdots, K\} \\
&m = 1, 2, \cdots, B \\
\mathbf{h}[m] &= \begin{bmatrix}\mathbf{h}_{I_k(2)}[m]^T & \mathbf{h}_{I_k(3)}[m]^T & \cdots & \mathbf{h}_K[m]^T\end{bmatrix}^T \\
\mathbf{h}_k[m] &= \begin{bmatrix}h_{k,0}[m] & k_{k,1}[m] & \cdots & h_{k,N_1}[m]\end{bmatrix}^T \\
\mathbf{w}[m] &= \begin{bmatrix}w_0[m] & w_1[m] & \cdots & w_{N_2}[m]\end{bmatrix}^T \\
\mathbf{\Phi}[m] &= \begin{bmatrix}\mathbf{U}_{I_k(2)}[m] & \mathbf{U}_{I_k(3)}[m] & \cdots & \mathbf{U}_K[m]\end{bmatrix} \\
\mathbf{\Xi}[m] &= \mathbf{U}_{I_k(1)}[m] \\
\mathbf{U}_k[m] &= \begin{bmatrix}\mathbf{u}_k[n_m] & \mathbf{u}_k[n_m+1] & \cdots & \mathbf{u}_k[n_m+M-1]\end{bmatrix}^T \\
\mathbf{u}_k[n_m] &= \begin{bmatrix}\tilde{\psi}_k[n_m] & \tilde{\psi}_k[n_m-1] & \cdots & \tilde{\psi}_k[n_m-(N_1;N_2)]\end{bmatrix}^T \\
\mathbf{e}_{(\chi)}[m] &= 1\times \\
&\quad \begin{bmatrix}e_{(\chi)}[n_m] & e_{(\chi)}[n_m+1] & \cdots & e_{(\chi)}[n_m+M-1]\end{bmatrix}^T
\end{aligned} \tag{6}$$

Here, $\mathbf{h}_k[m]; \mathbf{w}[m]$ denote the current $kth-$order DPD filter coefficients, and the digital SI cancellation filter coefficients, with memory depths of N_1 and N_2, respectively, n_m denotes the index of the first sample of the processing block m, and B denotes the total number of blocks utilized for the parameter learning. Furthermore, $\mathbf{e}_{(\chi)}[m]$ denotes the vector of error signal samples, with subscript $\chi \in \{\mathrm{Obs.RX}; \mathrm{MainRX}\}$ referring to the input either from the observation RX chain

TABLE I
THE COMPUTATIONAL COMPLEXITIES OF THE PROPOSED DPD FILTERING AND SI REGENERATION ALGORITHM, AND THE CORRESPONDING PARAMETER LEARNING STAGES.

Running complexity of DPD and SI regeneration (FLOP/sample)			Parameter learning complexity (FLOP/BM samples)	
Basis function generation	DPD filtering	Linear filtering for SI regeneration	DPD filters	Linear digital filter
$K+2$	$4(K-1)(N_1+1)-2$	$8N_2+6$	$B(K-1)(N_1+1)(4M+1)$	$B(N_2+1)(8M+2)$

or from the main RX chain. Thus, these error signal samples contain the TX leakage signal from the main RX chain under the cancellation filter parameters $\mathbf{w}[m]$, in the case of the RF canceller adaptation. On the other hand, in the case of the DPD adaptation, the error signal samples are the residual distortion at the PA output, under the DPD filter parameters $\mathbf{h}[m]$, which are calculated by subtracting the scaled observation signal at the PA output from the undistorted signal $x[n]$, as also explained in [16]. Consequently, the coefficients of the DPD filters and the SI cancellation filter are updated using the decorrelation-based block-adaptive algorithm as

$$\begin{aligned} \mathbf{h}[m+1] &= \mathbf{h}[m] - \mu_1 \left[\mathbf{e}_{\mathrm{Obs.RX}}[m]^H \mathbf{\Phi}[m]\right]^T \\ \mathbf{w}[m+1] &= \mathbf{w}[m] - \mu_2 \left[\mathbf{e}_{\mathrm{MainRX}}[m]^H \mathbf{\Xi}[m]\right]^T, \end{aligned} \tag{7}$$

where $\mu_1; \mu_2$ refer to the learning rate of the proposed block-adaptive algorithm, which can be chosen independently for the DPD and the cancellation filter coefficients, and provides a trade-off between the speed of convergence and stability of the algorithm.

B. Computational Complexity Analysis

One main advantage of the proposed technique is its reduced computational complexity compared to the existing nonlinear active RF cancellers, reported e.g. in [5], [10], [11]. Overall, the complexity of the proposed technique consists of the computational complexity of the DPD stage and the computational complexity of the active RF cancellation stage. The computational complexity of each of these two stages can be further divided into three main parts, namely, the adaptation complexity, the parameter learning complexity, and the running complexity.

The adaptation complexity refers to the processing required to adapt filter coefficients under new operating conditions arising due to the temperature changes, operating environment changes, or device aging. In general, the proposed parameter learning approach is capable of dynamically updating the coefficients due to any changes in the PA behavior or the passive isolation structure. However, it is interesting to note that the nonlinear behavior of the PA is considered slowly-varying compared to the characteristics of the SI coupling channel. Therefore, by separating the nonlinear DPD processing from the linear digital cancellation filter estimation, the proposed approach enables the DPD parameter adaptation to run intermittently at a slower-rate compared to the linear digital SI cancellation filter adaptation. In contrast, the existing nonlinear RF cancellers, such as [5], [10] and [11], require complex behavioral modeling for characterizing the nonlinear SI channel, due to co-existing PA nonlinearity and the coupling channel, and a wideband auxiliary TX chain to generate the RF cancellation signal. This leads to significant increase in the adaptation complexity and the power consumption of the RF canceller, compared to the proposed solution.

When it comes to the parameter estimation complexity, we wish to emphasize that the parameter learning for the DPD filters and the cancellation filter is done successively, and due to structural similarity in the parameter learning, the computing resources can be flexibly reused in an actual hardware implementation. The exact complexities in terms of floating point operations per an overall parameter learning sample size of $B \times M$ samples are given in Table I.

Finally, the running complexity for DPD processing and the SI regeneration is composed of two main parts: the complexity of the basis function generation, and the basis function filtering. We evaluate the complexity for performing these operations in terms of floating point operations (FLOP), and list them also in Table. I, while concrete numerical values are presented in Section IV.

IV. PERFORMANCE RESULTS

The performance of the proposed technique is evaluated and demonstrated in this section through extensive RF measurements. The measurement setup is shown in Fig. 2, while the relevant parameters are listed in Table. II. The measurement setup includes an Analog Devices evaluation board (AD9368-2), which is equipped with two RF transmitter chains, to generate main and auxiliary transmitter RF signals, and an observation receiver chain, to capture the PA output signal. In addition, a commercial LTE Band 1 BS PA (MD7IC2250GN) with an average output power of $+36$ dBm and a LNA (HD24089) with IIP3 of -7 dBm in the RX chain are adopted. The passive isolation is assumed to be 40 dB, achieved here through a cascaded of a circulator and an attenuator. The signal from the LNA output is fed to the RF input of the vector signal transceiver (NI PXIe-5645R), which acts as the main RX chain, and down-converts and digitizes the received signal. The processing sampling rate during the parameter estimation is 61.44 MHz. The presented results are plotted using a long realization of the transmit signal, with random subcarrier data symbols, after the proposed closed-loop learning system has converged.

Figs. 3(a) shows the LNA-input referred power spectral density (PSD) curves of the TX leakage signal before and after

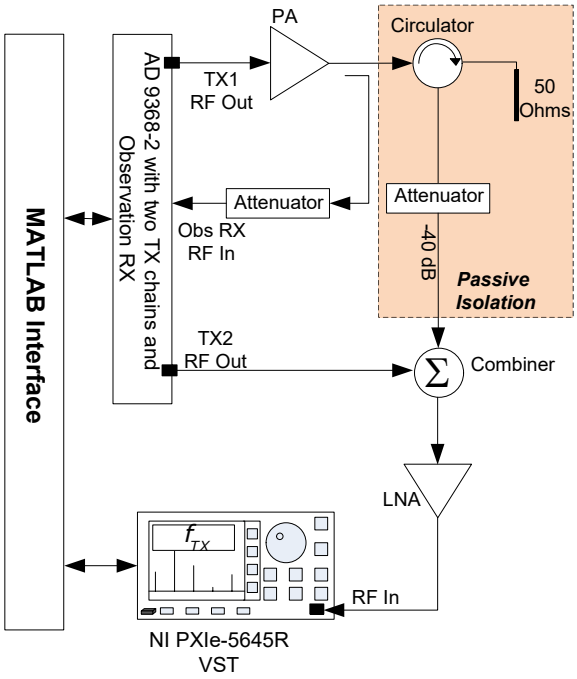

Fig. 2. Block diagram of the RF measurement setup used for evaluating the performance of the proposed technique.

TABLE II
THE ESSENTIAL MEASUREMENT PARAMETERS

Parameter	Value
TX signal bandwidth	20 MHz
TX waveform	OFDMA
TX signal subcarrier spacing	15 kHz
TX/RX center frequency	2.14 GHz
TX power	+35 dBm
SI power at LNA input	-5 dBm
LNA IIP3	-7 dBm
Parameter learning block size (M)	13 000
Total number of blocks used for parameter estimation (B)	20
DPD memory depth (N_1)	9
DPD nonlinearity order (K)	7
Digital cancellation filter length (N_2)	7

RF cancellation, with no DPD for PA linearization and when both the DPD and active RF canceller work in conjunction. In Fig. 3(b), the achievable active RF cancellation gain with and without TX PA linearization is plotted as a function of transmit power level. It is evident from these figures that there are strong PA-induced nonlinear distortion products appearing in the TX leakage signal when PA linearization is not used. Consequently, the residual SI level is still relatively strong when only linear SI cancellation is pursued. However, when both the PA linearization and linear SI cancellation are deployed, substantial SI suppression is achieved, leaving the residual SI only some 20 dB away from the thermal noise floor. In the IBFD transceiver, such residual SI can be suppressed using the digital cancellers in the transceiver digital front-end, such as the ones described in [18], [19].

Another important finding is that the proposed parameter learning technique is immune to the LNA-induced distortion. In order to test and verify the cancellation performance of the proposed technique in a rigorous manner, we have deliberately adopted a highly nonlinear LNA in the RX chain in our experiments. The TX leakage signal, being -5 dBm at the LNA input without RF cancellation, implies that the observed RX signal in the starting phase of linear digital SI cancellation filter parameter learning will contain severe nonlinear LNA-induced distortion. However, the proposed closed-loop parameter estimation and cancellation algorithm facilitates accurate parameter estimation, as the leakage signal power at the LNA input decreases iteratively in each algorithm iteration while the algorithm converges to the optimum coefficients, and consequently the LNA-induced distortion becomes negligibly small. This is a highly desirable property of the proposed closed-loop learning algorithm as it can offer enhanced cancellation performance while allowing the use of nonlinear RF components. Altogether, the proposed DPD and linear RF canceller can suppress the SI by approximately 50 dB, representing state-of-the-art in active RF cancellation literature.

Complexity-wise, the overall running complexity in DPD filtering and SI regeneration is 19 giga-FLOP per second (GFLOP/s), while the parameter learning complexity for DPD filters and digital cancellation filter is 63 mega-FLOP (MFLOP) and 8 MFLOP, respectively, both of which are indeed within the processing capabilities of modern base station radio transceivers. For reference, the involved processing complexity to achieve similar SI cancellation performance with a nonlinear RF canceller, e.g. the one reported in [5], is 40 GFLOP/s for the SI regeneration and 143 MFLOP for the parameter learning. Therefore, it can be concluded that the overall complexity can indeed be reduced significantly through the proposed hybrid DPD and linear SI cancellation.

Finally, there is still some residual SI after active RF cancellation which, as mentioned earlier, can be further suppressed by employing a purely digital canceller. However, the SI also contains the transmitter noise from the main and auxiliary transmitter chains, which cannot be fully cancelled by the digital canceller. Nevertheless, the impact of transmitter noise can be minimized through careful RF design practices, as investigated thoroughly in [5], or alternatively by employing digital cancellation methods that use the PA output signal as a reference signal [13], [14].

V. CONCLUSIONS

A digitally-assisted active RF cancellation scheme with closed-loop parameter learning was proposed for suppressing the SI in simultaneous transmit-receive systems. In the proposed scheme, the nonlinear distortion in the transmit signal are suppressed through digital pre-distortion. Then, a baseband equivalent replica of the true SI is created in the transceiver digital front-end, through linear filtering of the transmit data. The actual RF cancellation signal is generated in the auxiliary TX chain, which is finally added to the received signal at the RX LNA input in order to suppress the SI.

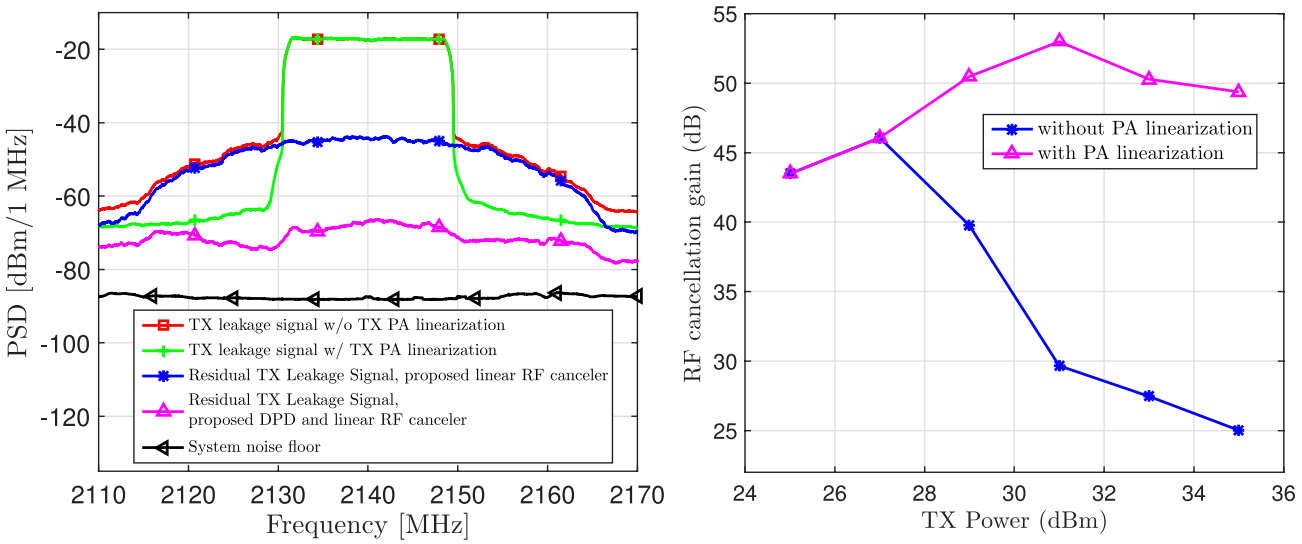

(a) (b)

Fig. 3. The performance results of the proposed technique at +35 dBm TX power and with 40 dB passive isolation. TX signal bandwidth is 20 MHz. (a) measured signal power spectral density curves referred to LNA input with and without active RF cancellation ; (c) measured RF cancellation gain against different TX power with and without TX PA linearization.

Furthermore, we presented a closed-loop decorrelation-based algorithm for efficiently estimating both the nonlinear DPD filters and the linear digital cancellation filter coefficients in a flexible manner. The RF measurement results indicate excellent suppression of the SI, while the computational complexity analysis further demonstrated that the involved complexity is lower than the corresponding complexities of state-of-the-art techniques. Hence, the proposed technique can significantly enhance the TX-RX isolation in future simultaneous transmit-receive radio devices with nonlinear TX and RX chain RF components, thus facilitating flexible spectrum allocation and utilization in, e.g., future 5G radio networks.

REFERENCES

[1] A. Sabharwal, P. Schniter, D. Guo, D. W. Bliss, S. Rangarajan, and R. Wichman, "In-band full-duplex wireless: challenges and opportunities," *IEEE J. Sel. Areas Commun.,* vol. 32, no. 9, pp. 1637-1652, Sep. 2014.

[2] D. Korpi, "Full-duplex wireless: Self-interference modeling, digital cancellation, and system studies," Ph.D. dissertation, Tampere University of Technology, Dec. 2017.

[3] D. Bharadia, E. McMilin, and S. Katti, "Full duplex radios," *ACM Special Interest Group Data Commun. Comput. Commun. Rev.,* vol. 43, no. 4, pp. 375-386, Aug. 2013.

[4] S. Hong *et al.*, "Applications of self-interference cancellation in 5G and beyond," *IEEE Commun. Mag.*, vol. 52, no. 2, pp. 114-121, Feb. 2014.

[5] A. Kiayani *et al.*, "Adaptive nonlinear RF cancellation for improved isolation in simultaneous transmit-receive systems," *IEEE Trans. Microw. Theory Techn.*, vol. 66, no. 5, pp. 2299-2312, May 2018.

[6] M. Duarte and A. Sabharwal, "Full-duplex wireless communications using off-the-shelf radios: feasibility and first results," in *Proc. Asilomar Conf. Signals Syst. Comput.,* 2010, pp. 1558-1562.

[7] S. Ahmed, R. Eslampanah, R. A. Antiohos, S. Andersson, and M. Faulkner, "Baseband equalizer for TX leakage cancellation in active duplexing," in *Proc. Signal Process. Commun. Syst.*, 2015, pp. 1-4.

[8] J.-H. Lee, "Self-interference cancelation using phase rotation in full-duplex wireless," *IEEE Trans. Veh. Technol.*, vol. 62, no. 9, 917 pp. 4421-4429, Nov. 2013.

[9] L. Anttila, *et al.*, "Cancellation of power amplifier induced nonlinear self-interference in full-duplex transceivers," in *Proc. Asilomar Conference on Signals, Systems and Computers,* 2013, pp. 1193-1198.

[10] R. Askar, T. Kaiser, B. Schubert, T. Haustein and W. Keusgen, "Active self-interference cancellation mechanism for full-duplex wireless transceivers," in *Proc. 9th Intl. Conf. on Cognitive Radio Oriented Wireless Networks and Communications (CROWNCOM)*, 2014, pp. 539-544.

[11] Y. Liu, X. Quan, W. Pan, and Y. Tang, "Digitally assisted analog interference cancellation for in-band full-duplex radios," in *IEEE Communications Letters,* vol. 21, no. 5, pp. 1079-1082, May 2017.

[12] B. Debaillie *et al.*, "Analog/RF solutions enabling compact full-duplex radios," *IEEE J. Sel. Areas Commun.*, vol. 32, no. 9, pp. 1662-1673, Sep. 2014.

[13] Y.-S. Choi and H. Shirani-Mehr, "Simultaneous transmission and reception: algorithm, design and system level performance," *IEEE Trans. Wireless Commun.,* vol. 12, no. 12, pp. 5992-6010, Dec. 2013.

[14] T. Huusari, Y.-S. Choi, P. Liikkanen, D. Korpi, S. Talwar, and M. Valkama, "Wideband self-adaptive RF cancellation circuit for full-duplex radio: Operating principle and measurements," in Proc. *IEEE 81st Veh. Technol. Conf. (VTC-Spring)*, May 2015, pp. 1-7.

[15] J. Zhou, T. H. Chuang, T. Dinc, and H. Krishnaswamy, "Integrated wideband self-interference cancellation in the RF domain for FDD and full-duplex wireless," *IEEE J. Solid-State Circuits*, vol. 50, no. 12, pp. 3015-3031, Dec. 2015.

[16] M. Abdelaziz *et al.*, "Decorrelation-based concurrent digital predistortion with a single feedback path," *IEEE Trans. Microw. Theory Techn.*, vol. 66, no. 1, pp. 280-293, Jan. 2018.

[17] S. S. Haykin, *Adaptive Filter Theory*, 3rd ed. Upper Saddle River, NJ, USA: Prentice-Hall, 2002.

[18] D. Korpi *et al.*, "Full-duplex mobile device: pushing the limits," *IEEE Communications Magazine*, vol. 54, no. 9, pp. 80-87, September 2016.

[19] D. Korpi, Y. S. Choi, T. Huusari, L. Anttila, S. Talwar, and M. Valkama, "Adaptive nonlinear digital self-interference cancellation for mobile inband full-duplex radio: Algorithms and RF measurements," in Proc. *IEEE Global Commun. Conf. (GLOBECOM)*, Dec. 2015, pp. 1–7.